A Human-Specific α7-Nicotinic Acetylcholine Receptor Gene in Human Leukocytes: Identification, Regulation and the Consequences of *CHRFAM7A* Expression

Todd W Costantini,[1] Xitong Dang,[1,2*] Maryana V Yurchyshyna,[1] Raul Coimbra,[1] Brian P Eliceiri,[1] and Andrew Baird[1]*

[1]Department of Surgery, University of California San Diego Health Sciences, San Diego, California, United States of America; and [2]Cardiovascular Research Center, Luzhou Medical College, Luzhou, Sichuan, China

The human genome contains a variant form of the α7-nicotinic acetylcholine receptor (α7nAChR) gene that is uniquely human. This *CHRFAM7A* gene arose during human speciation and recent data suggests that its expression alters ligand tropism of the normally homopentameric human α7-AChR ligand-gated cell surface ion channel that is found on the surface of many different cell types. To understand its possible significance in regulating inflammation in humans, we investigated its expression in normal human leukocytes and leukocyte cell lines, compared *CHRFAM7A* expression to that of the *CHRNA7* gene, mapped its promoter and characterized the effects of stable *CHRFAM7A* overexpression. We report here that *CHRFAM7A* is highly expressed in human leukocytes but that the levels of both *CHRFAM7A* and *CHRNA7* mRNAs were independent and varied widely. To this end, mapping of the *CHRFAM7A* promoter in its 5′-untranslated region (UTR) identified a unique 1-kb sequence that independently regulates *CHRFAM7A* gene expression. Because overexpression of *CHRFAM7A* in THP1 cells altered the cell phenotype and modified the expression of genes associated with focal adhesion (for example, FAK, P13K, Akt, rho, GEF, Elk1, CycD), leukocyte transepithelial migration (Nox, ITG, MMPs, PKC) and cancer (kit, kitL, ras, cFos cyclinD1, Frizzled and GPCR), we conclude that *CHRFAM7A* is biologically active. Most surprisingly however, stable *CHRFAM7A* overexpression in THP1 cells upregulated *CHRNA7*, which, in turn, led to increased binding of the specific α7nAChR ligand, bungarotoxin, on the THP1 cell surface. Taken together, these data confirm the close association between *CHRFAM7A* and *CHRNA7* expression, establish a biological consequence to *CHRFAM7A* expression in human leukocytes and support the possibility that this human-specific gene might contribute to, and/or gauge, a human-specific response to inflammation.

INTRODUCTION

In 1979, Richman described the presence of a functionally distinct nicotinic acetylcholine receptor (AChR) on human lymphocytes that appeared to have altered ligand binding (1). As recently reviewed by Costantini *et al.* (2) and Sinkus *et al.* (3), it was almost twenty years later that Gault *et al.* (4) sequenced the human α7nAChR gene on chromosome 15q13–14 and found it to be structurally similar to that of all other species. At the same time, however, they noted the presence of a second, human-specific partially duplicated α7nAChR-like gene that localized 1.6 Mb 5′ upstream from human *CHRNA7* (4). With only 386 amino acids of the α7nAChR channel domain, this new human-specific gene was initially called dupα7nAChR and found to encode an amino terminus that originated from a kinase gene on chromosome 3 (5). The ultimate genetic rearrangement, which occurred after the divergence of humans from other primates (6,7), created a new, distinct and human-specific open reading frame (ORF) that produces an exclusively human α7nAChR now called *CHRFAM7A* (8). Many species, including human, great apes, mice and rats have orthologs of *CHRNA7* that are generated by alternative splicing of their respective *CHRNA7* mRNA. However, only the human genome has a distinct

---

*TWC and XD contributed equally to the work presented in this study.

Address correspondence to *Andrew Baird, Division of Trauma, Surgical Care, Burns, and Acute Care Surgery, Department of Surgery, University of California San Diego Health Sciences, 212 Dickinson Street, MC 8236, San Diego, CA 92103. Phone: 619-471-9027; Fax: 619-543-2325; E-mail: anbaird@ucsd.edu.*

CHRFAM7A gene that can gauge the function and ligand tropism of the normal α7nAChR ligand-gated channel (3,9).

Since its discovery in 1998, *CHRFAM7A* has largely been the focus of neuroscience and mental health research because historically the α7nAChR was viewed as a neuron-specific, ligand-gated ion channel. More recently, however, its detection in normal human leukocytes (10,11) has gained particular attention because several *in vitro* studies have shown that *CHRFAM7A* modifies α7nAChR channel activity and changes ligand tropism (12–14). Because α7nAChR activation is closely tied to the inflammatory responses of peripheral tissues, these observations raise the possibility that *CHRFAM7A* may be particularly relevant to gauging inflammation in humans. The Tracey laboratories, for example, established that efferent signaling of the vagus nerve acts exclusively via α7nAChR activation in the spleen to regulate systemic cytokine responses to infection in mice (15–20). Similarly, Costantini and colleagues demonstrated the existence of a similar α7nAChR-dependent regulation of the local inflammatory response in tissues (21–27). With α7nAChR activation clearly essential to inflammation, not to mention vagus nerve responsiveness and leukocyte function (28,29), we reasoned that it was therefore critical to understand how a human-specific α7nAChR in human leukocytes might influence human leukocyte function, the regulation of its expression and the biological consequences of its expression. Because newly evolved genes such as *CHRFAM7A* disproportionately segregate with complex human disease (30,31), the results point to the possible existence of human-specific responses to inflammation that are not present in other species. If so, *CHRFAM7A* may gauge the α7nAChR-mediated effects of the human vagus nerve.

MATERIALS AND METHODS

Materials

The plasmid encoding the full-length *CHRFAM7A* (variant 1: NM_139320.1) was from OriGene (Rockville, MD, USA) and differs from a shorter *CHRFAM7A* (variant 2: NM_148911) in that it encodes a 90-amino-acid amino terminus containing the FAM7A sequence (NH2-MQKYCIYQHF QFQLLIQHLW IAANCDI) and a α7nAChR amino terminus peptide (ADE RFDATFHTNV LVNSSGHCQY LPPGIFKSSC YIDVRWFPFD VQHCKLKFGS WSYGGWSLDL). The plasmid encoding full-length *CHRNA7* (variant 2: NM_001190455) was from GeneCopoeia (Rockville, MD, USA) and differs from the shorter *CHRNA7* (variant 1: NM_000746*)* by codons that encode a GKATASPPSTPPWDPGHIPGASVRPAPGP peptide introduced at His[18] of the α7nAChR subunit. The pGL4 promoterless expression plasmid encoding firefly luciferase was purchased from Promega (Madison, WI, USA). All other chemicals and reagents were the products of Sigma-Aldrich (St. Louis, MO, USA) unless specified otherwise.

Human Peripheral Leukocytes

Informed consent was obtained from healthy volunteers for the collection of peripheral blood. Volunteers were recruited and enrolled by the University of California San Diego (UCSD) Clinical Translational Research Institute (San Diego, CA, USA). Venous blood was collected by peripheral venipuncture in BD Vacutainer blood collection tubes containing ethylenediaminetetraacetic acid (EDTA) (BD Biosciences, San Jose, CA, USA) and placed on ice. Red blood cells were lysed using BD Pharm Lyse ammonium chloride solution (BD Biosciences) at room temperature for 15 min and leukocytes pelleted by centrifugation. Cell pellets were stored at –80°C until further analyses. The UCSD Institutional Review Board approved the enrollment of participants, consent forms and specimen collection protocols.

Cell Culture

All cell lines were originally purchased from ATCC (Manassas, VA, USA) and/or acquired through the UCSD Department of Surgery, Division of Trauma, Burns and Acute Care Surgery Cell Repository (San Diego, CA, USA). Thawed cells were washed in RPMI culture media containing 10% fetal calf serum (FCS), the pellet reconstituted in culture media and cells plated into six-well tissue culture plates. All cells were washed 48 h later and allowed to grow to 90% confluence and propagated with trypsin digestion as needed. For transduction studies, cells were seeded at 2×10^6 in 6-well tissue culture plates the day before the experiment. As indicated in each experiment, cells were harvested directly from the culture dishes for total RNA preparation, processed for stable or transient transfection or treated with 100 ng/mL LPS (L4391, Sigma-Aldrich) for 3 h. At the end of incubations, cells were harvested, total RNA isolated and the cDNA generated (see below) used for analyses of gene expression.

Lentivirus Constructs for *CHRFAM7A* Expression

The ORF of human *CHRFAM7A* (variant 1) was amplified by PCR from the *CHRFAM7A*-pCMV6-Entry plasmid (PS100001, OriGene, Rockville, MD, USA) using: forward primer: 5′-aGTcC TCGAGATGcaaaaatattgcatct-3′; reverse primer: 5′-attcGGATCCTTACGCAAAG TCTTTGGACACGGC-3′.

The PCR products were purified and cloned into the bicistronic pLVX-IRES-ZsGreen1 lentivirus plasmid as recommended by the manufacturer. The identity of the plasmid was confirmed by DNA sequencing (Retrogen, San Diego, CA, USA). Lentivirus was packaged using the Lenti-X HTX Packaging System (631247, Clontech, Mountain View, CA, USA) following vendor instructions. After 48 h, the supernatant containing virus was collected and used to transduce THP1 cells. Stable transfected green fluorescent protein (GFP)-positive THP1 cells were detected by fluorescence microscopy and purified by cell sorting. Cells were expanded without further selection and the stability of transduction monitored by weekly flow cytometry.

Flow Cytometry and Cell Sorting of THP1 Cells

For flow cytometry analyses, cells were washed and fixed with Cytofix according to the manufacturer's recommendations (BD Biosciences) for 10 min on ice. Cells were then incubated with labeled bungarotoxin (BD Biosciences) in FACS buffer (1% bovine serum albumin [BSA] in phosphate buffered saline [PBS] containing 0.005% sodium azide) and washed in FACS buffer. Flow cytometry was performed with a Becton Dickinson FACSCalibur and data analysis performed with CellQuestPro software from Becton, Dickinson and Company (BD) (Franklin Lakes, NJ, USA), processed and analyzed using JFlow. To purify GFP-expressing THP1 cells, the transduced cells were sorted twice by FACS at the core facilities of the Center for AIDS Research at UCSD, selected for GFP expression and expanded as cell suspensions. Stable expression was monitored weekly for retention of > 85% cells expressing GFP as measured by flow cytometry. Cells were propagated in 10% RPMI1640.

RNAseq, Gene Expression and Pathway Analyses

Total RNA was prepared from transduced and sorted THP1 cells using RNeasy kit (Qiagen, San Diego, CA, USA) and was quantified using a NanoDrop Spectrophotometer (Thermo Fisher Scientific Inc., Waltham, MA, USA). One μg total RNA was used for RNAseq analyses and performed by contract with the Genomics Core, Cedars-Sinai Medical Center (Los Angeles, CA, USA). Bioinformatic analyses, differential gene expression and pathway analyses were performed by contract with Accura-Science (Johnston, IA, USA). For datasets and RNA-seq differential expression (DE) analysis, the BAM files for vector- and stable *CHRFAM7A*-transduced cells were generated by RNA-seq at the genome core facilities at Cedars-Sinai Genomics core at Cedars Sinai Medical Center and were used for differential gene expression analyses. Comparisons were made between *CHRFAM7A* and

vector using two methods to define differentially expression genes. DESeq (32) is one of the few methods suitable with limited replicates (33) and controls for false positive signals (34,35). The Python package HTseq was used to produce the count table and a *P* value <0.05 was set as cutoff. In the second method, the results of DESeq were overlapped with Cuffdiff (36) and a *P* value <0.05 was chosen as cutoff. The differentially expressed gene groups defined by both analytical methods were for functional enrichment analysis and GOseq in bioconductor was used for gene ontology analysis (37) with up- and downregulated differentially expressed genes respectively. A *P* value cutoff of 0.05 was used to choose significant gene ontology (GO) terms. The Functional Class Scoring method implemented in GSEABase was used for Kyoto Encyclopedia of Genes and Genomes (KEGG) pathway analyses (38) and a *P* value of <0.05 was used to define significant pathway categories.

Isolation of RNA from Cultured Cells and Preparation of cDNA for PCR and qPCR

Total RNA was prepared from cell lysates using the RNeasy kit and was quantified using a NanoDrop Spectrophotometer. One μg of the total RNA was reversed transcribed using iScript cDNA synthesis kit (Bio-Rad, San Diego, CA, USA) in a 20 μL reaction as described by the manufacturer and 1 μL was used for RT-PCR or real-time qPCR analyses.

RT-PCR and Quantitative RT-PCR for *CHRFAM7A* and CHRNA7

RT-PCR was performed in a 50 μL reaction containing 45 μL PCR blue mix (Invitrogen [Thermo Fisher Scientific]), 1 μL of each primer (10 μmol/L), 1 μL cDNA and 2 μL water. The cycling conditions were 94°C for 4 min followed by 35 cycles of 94°C for 30 s, 60°C for 30 s and 72°C for 60 s and a final extension at 72°C for 5 min. Ten μL of each PCR product were resolved on a 2% agarose gel and images were acquired using an Alpha Innotech imaging system (Fisher

Scientific [Thermo Fisher Scientific]). Real-time qPCR was performed in a 25 μL reaction containing 12.5 μL 2× SYBR Green PCR Master Mix (Bio-Rad), 0.5 μL of each primer (10 μmol/L), 1 μL cDNA and 10.5 μL water. PCR cycling conditions were: 95°C for 10 min followed by 45 cycles of 94°C for 25 s, 60°C for 25 s and 72°C for 40 s. Primer efficiency for *CHRFAM7A* and *CHRNA7* were 100% and 94% respectively.

Primers for *CHRFAM7A* were: sense, 5′-ATAGCTGCAAACTGCGATA-3′; antisense, 5′-cagcgtacatcgatgtagcag-3′. Primers for *CHRNA7* were: sense, 5′-acATGcgctgctcgccggga-3′; antisense, 5′-gattgtagttcttgaccagct-3′. Primers for *GAPDH* were: sense, 5′-CATGAGAAGT ATGACAACAGCCT-3′; antisense, 5′-AGTCCTTCCACGATACCAAAGT-3′.

5′ RACE and Identification of *CHRFAM7A* Variant 1

5′ RACE was performed using SMARTer RACE cDNA Amplification Kit (Clontech) following vendor's instructions. Briefly, total RNA was prepared from THP1 cell with RNeasy kit (Qiagen). Three μg total RNA was processed for mRNA using PolyA Spin mRNA Isolation Kit (New England Biolabs [NEB], Ipswich, MA, USA). One-fifth of the poly A mRNA was reverse transcribed and the resulting cDNA was amplified sequentially by PCR and nested PCR. Both gene-specific primers (GSP), GSP and nestGSP listed below, hybridize to the fifth exon of human *CHRNA7/ CHRFAM7A*, with nestGSP 5′ to the GSP without overlapping. The nested PCR products were purified and cloned into pDrive (Qiagen). Colonies were sequenced to identify the 5′ initiation sites and the 5′ sequence upstream the fifth exon of *CHRNA7/CHRFAM7A* (GSP [5′-GCAGG TACTGGCAATGCCCAGAAG-3′], NestGSP [5′-TAGTGTGGAATGTGG CGTCAAAGCG-3′]).

Analyses of the *CHRFAM7A* Promoter

The putative *CHRFAM7A* promoter region spanning from –2363 to +22 relative to the open reading frame ATG start codon was amplified by PCR of genomic

DNA isolated from HEK293 cells. The longest fragment was cloned into pGL4 promoterless luciferase reporter plasmid (Promega) according to the manufacturer's specifications and the resulting plasmid, pGL4-*CHRFAM7A* (~2400 bp), was confirmed by DNA sequencing and thereafter referred to as f2400 to reflect its size.

The primers were: sense, 5′-ATCAGCTAGCTCTAGATAGACAGCATTTTA-3′ containing a *Nhe*I restriction site; antisense, 5′-GCATAGATCTGGTAGATGCAATATTTTTGCAT-3′ containing a *Bgl*II restriction site.

Three serial 5′ deletion promoter constructs of 1800, 1000 and 500 bp were derived by PCR of the f2400 template using the same antisense primer described above, with one of three sense primers to obtain: f1800 (5′-ATCAGCTAGCAAGCCTTCATCAGTGGAAAT-3′); f1000 (5′-ATCAGCTAGCGTATGACTCAAGTCCTTGAC-3′); f500 (5′-ATCAGCTAGCCTTGCTGTATTCTCTAAACTA-3′).

The fragments generated were cloned into the pGL4 vector to create plasmids f1800, f1000 and f500, which were each sequenced to confirm their identity. These plasmids were then transiently transfected into THP1 cells as described below and luciferase activity was analyzed 30 h after transfection following the manufacturer's instructions (Promega). Luciferase activity was normalized to protein concentration and the data presented as relative luciferase activity compared with the activity of promoterless pGL4 transfected cells.

Transfections of THP1 Cells for Promoter Analyses

THP1 cells, cultured in RPMI1640 supplemented with 1× GlutaMAX (Life Technologies [Thermo Fisher Scientific]) and 1× penicillin/streptomycin, were seeded at 5×10^5 per well in a 24-well plate 2 h before transfection. Transient transfection was performed using Lipofectamine 2000 (Invitrogen [Thermo Fisher Scientific]). Briefly, 2.5 μL of the Lipofectamine 2000 was added into 50 μL OPTI-MEM (Invitrogen [Thermo

Fisher Scientific]), vortexed for 5 s and then continued to incubate at room temperature for 5 min. One μg plasmid diluted into 50 μL OPTI-MEM was added into the above mixture, vortexed for 5 s and incubated at room temperature for 20 min. The DNA-complex was then added dropwise to cells and cells were incubated for 30 h. Cells were washed with PBS and lysed with 100 μL Passive Lysis buffer at room temperature for 30 min with shaking. The lysate was spun down and 10 μL of the supernatant was used for luciferase assay on POLARstar Omega plate reader (BMG Labtech, Cary, NC, USA). Luciferase activity normalized to protein concentration was expressed as fold changes over that of pGL4-transfected cells.

Statistical Analyses

CHRNA7 and *CHRFAM7A* gene expression were normalized to that of *GAPDH* and the fold changes calculated by ΔΔCt method using the relative expression software tool (REST) for groupwise comparisons and statistical analyses of relative expression results (39). The GraphPad (GraphPad Software Inc., La Jolla, CA, USA) program Prism 6 was used for other analyses including two-tailed unpaired *t* test, Wilcoxon signed rank test of unpaired *t* test and analysis of variance (ANOVA) as indicated in the text and in legends to the figures.

All supplementary materials are available online at www.molmed.org.

RESULTS

Detection of *CHRFAM7A* and CHRNA7 Expression in Human Leukocytes

During analysis of human-specific gene expression in leukocytes purified from the blood of normal volunteers, we examined whether we could specifically detect concomitant expression of mRNAs encoding *CHRFAM7A* and *CHRNA7* (Figure 1). As described in Materials and Methods and illustrated in Figure 1A, the full-length *CHRFAM7A* (variant 1, NM_139320.1) differs from the shorter

CHRFAM7A (variant 2, NM_148911) in that it encodes a unique FAM7A peptide sequence (NH2-MQKYCIYQHF QFQLLIQHLW IAANCDI). Accordingly, PCR primers could be designed to specifically hybridize with *CHRFAM7A* variant 1. Because the *CHRFAM7A* variant 2 mRNA does not contain unique sequences that allow it to be differentiated from either *CHRFAM7A* (variant 1) or *CHRNA7* (see Figure 1A), no specific RT-PCR primers could be designed to detect *CHRFAM7A* (variant 2) so we used 5′ RACE (see below).

In contrast, the full-length *CHRNA7* mRNA (variant 2: NM_001190455) differs from the shorter *CHRNA7* mRNA (variant 1: NM_000746) by encoding a GKATASPPSTPPWDPGHIPGASVRP APGP peptide that allows both transcripts differentiated by size when analyzed by gel electrophoresis (see Figure 1A). They are also measured simultaneously by quantitative RT-PCR. As shown in Figure 1B, PCR of leukocyte cDNA prepared from the mRNA of seven volunteers established the presence of *CHRFAM7A* mRNA in all samples (see Figure 1B). *CHRNA7* was readily detected in four of seven samples (Figure 1C) and in all samples with longer exposures (not shown). Increased PCR cycle numbers showed ubiquitous expression of *CHRNA7*. Interestingly, leukocytes from different individuals appeared to express different combinations of *CHRNA7* variants 1 and 2. For example, three samples (lanes 3, 4 and 7) had the longer *CHRNA7* variant 1 transcript while a fourth (lane 4) only had variant 2 (see Figure 1C). Because no difference in the signal was obtained in the analyses of *GAPDH* (Figure 1D), the results suggest significant individual variability in expression of both leukocyte *CHRNA7* and *CHRFAM7A*. On average, however, the differences detected between the levels of both genes are not statistically different in normal human leukocytes (Figure 1E). Both *CHRNA7* and *CHRFAM7A* gene expression is markedly variable, ranging from 100 to 20,000 copies/μg of starting mRNA. Any differences in the
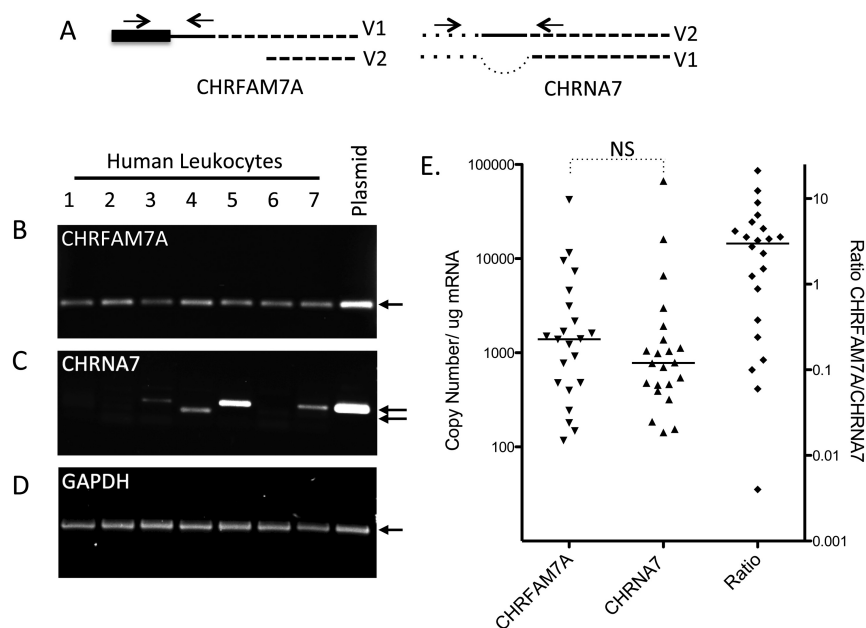
Figure 1. Expression of *CHRNA7* and *CHRFAM7A* in human leukocytes. In humans, there are two reported variants of both *CHRFAM7A* and *CHRNA7* and the PCR primers can help distinguish the longer variant 2 from variant 1 of *CHRNA7* based on size (A), they do detect or differentiate variant 2 of *CHRFAM7A*. RT-PCR of mRNA from human leukocytes cells isolated from 7 patients (lanes 1–7) was used to identify the presence of (B) the duplicate α7-nicotinic acetylcholine receptor (*CHRFAM7A*), (C) the human α7-nicotinic acetylcholine receptor (*CHRNA7*) or (D) *GAPDH* mRNA. Arrows show the expected size of the amplified sequence from the cognate plasmids. (E) This panel shows the results from quantitative RT-PCR for both *CHRFAM7A* and *CHRNA7*. Concentrations were determined against a plasmid standard curve generated for each gene and then expressed as copy number/μg of total mRNA amplified in the starting material. (NS = nonsignificant using two-tailed unpaired *t* test).

ratio *CHRFAM7A* and *CHRNA7* gene expression, which ranges as much as 10,000-fold between different donors (N = 22), is most striking when paired expression of *CHRFAM7A* to *CHRNA7* is assessed although the mean differences suggest that as much *CHRFAM7A* is expressed as *CHRNA7*, on average.

Identification of the *CHRFAM7A* Variant 1 mRNA Transcript in THP1 Cells

The 5′ RACE method was used to extend the *CHRFAM7A* cDNA clones from THP1 cells to detect *CHRFAM7A* variant 1 (see above) and to identify the 5′ UTR sequences of the corresponding *CHRFAM7A* mRNAs that might regulate gene expression. As shown in Figure 2A, we were able to identify several

CHRFAM7A variant 1 transcripts expressed in THP1 cells but did not detect variant 2. We detected four transcription initiation sites at –94, –206, –356 and –446 bp 5′ to the *CHRFAM7A* ORF. This sequencing also allowed us to deduce the primary sequence of leukocyte *CHRFAM7A* protein (Figures 2B, D), which demonstrated that it is identical to the variant 1 that is published in public genomic databases. These data also established the difference with the protein encoded by the *CHRNA7* gene (Figure 2C). Finally, the use of 5′ RACE allowed us to focus on 5′ untranslated region (5′ UTR) sequences that are responsible for the start of *CHRFAM7A* transcription and the potential promoter elements regulating *CHRFAM7A* gene expression.

CHRFAM7A and CHRNA7 Gene Expression in Leukocyte Cell Lines

We used RT-PCR to survey the expression of both *CHRFAM7A* and *CHRNA7* in human leukocyte lines (Figure 3). We found that HL60, RPMI-2286, U937, HEL92, Jurkat and ARH77 are like the premonocytic THP1 cell line and express both *CHRFAM7A* (Figure 3A) and *CHRNA7* (Figure 3B) when compared with *GAPDH* (Figure 3C). As in normal leukocytes (see Figure 1), we detect both variant 1 and variant 2 mRNA transcripts of *CHRNA7* (see Materials and Methods) depending on the cell evaluated. This raises the possibility that heteropentameric α7nAChRs exists on the leukocyte cell surface containing up to three distinct subunits: *CHRNA7* variant 1; CHRNA7 variant 2; and *CHRFAM7A*. Three cell lines (HL60, HEL92 and Jurkat) express both transcripts 1 and 2 of *CHRNA7* while U937 cells only express transcript 2 of *CHRNA7*. Three other cells (RPM-I2286, RH77 and THP1 cells) only express transcript 1 of *CHRNA7*. We conclude that significant heterogeneity of the α7nAChR subunits that compose the final cell surface pentameric channel may exist on the human leukocyte cell surface.

There are no antibodies that can distinguish the different molecular forms of *CHRNA7* and *CHRFAM7A*. Accordingly, we used qRT-PCR to quantify the expression of both *CHRNA7* (Figure 3D) and *CHRFAM7A* (Figure 3E) in the different leukocyte cell lines. Because HL60 cells appear to express equal amounts of variants 1 and 2 of *CHRNA7* (see Figure 3B) and intermediate amounts of *CHRFAM7A* (see Figure 3A), the expression levels of both genes were normalized to the levels detected in HL60 cells. As shown in Figure 3F, no consistent pattern was observed in the ratio of *CHRFAM7A* to *CHRNA7* which varied 10-fold to 10,000-fold higher in some cells (for example, HL-60, U937, HEL92 and THP1 cells) but were either near equal in others (RPMI-2286 cells) or 10 to 100 lower, for example in Jurkat and ARH77 cells. If mRNA ex-
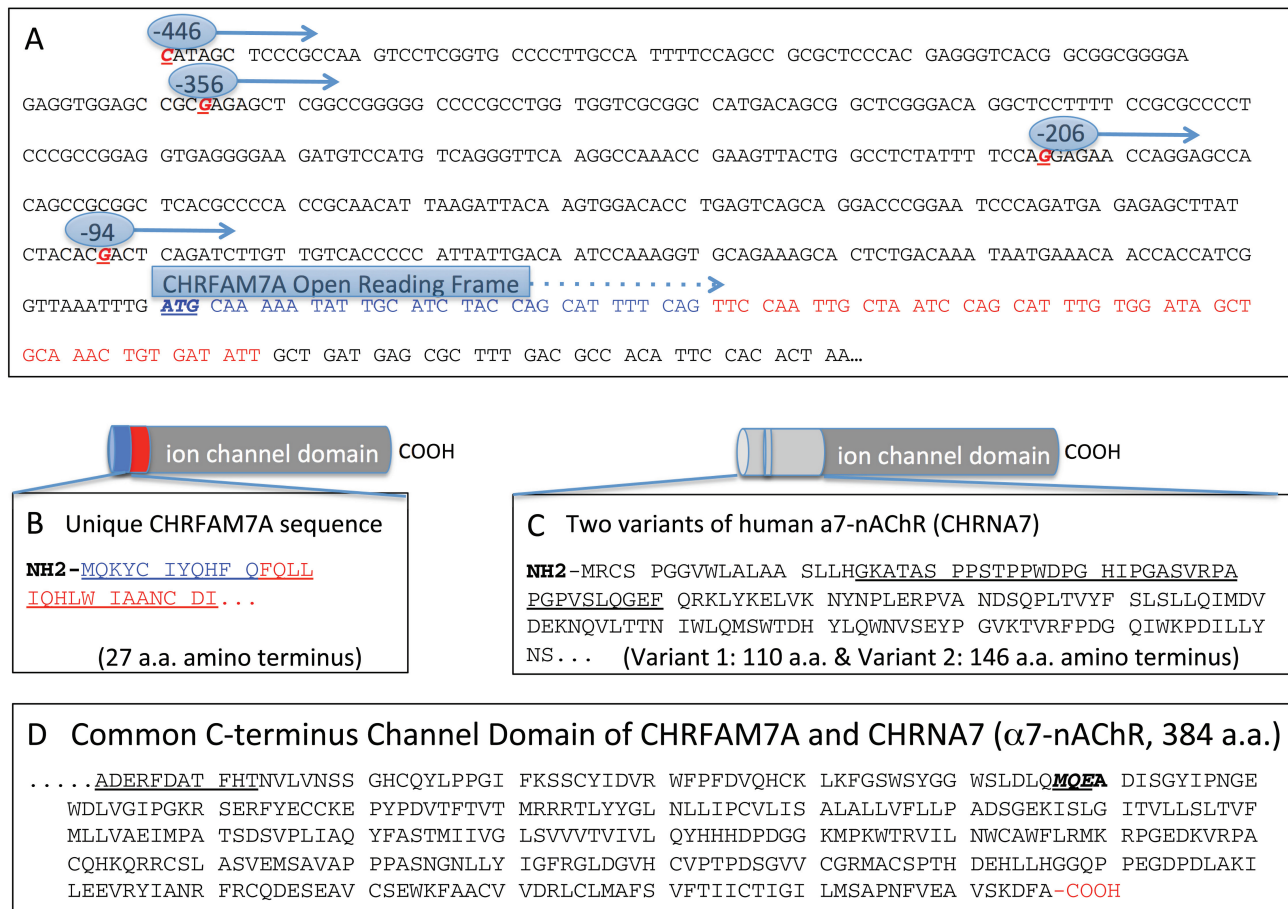
A -446
CATAGC TCCCGCCAA GTCCTCGGTG CCCCTTGCCA TTTTCCAGCC GCGCTCCCAC GAGGGTCACG GCGGCGGGGA
-356
GAGGTGGAGC CGC***G***AGAGCT CGGCCGGGGG CCCCGCCTGG TGGTCGCGGC CATGACAGCG GCTCGGGACA GGCTCCTTTT CCGCGCCCCT
-206
CCCGCCGGAG GTGAGGGGAA GATGTCCATG TCAGGGTTCA AGGCCAAACC GAAGTTACTG GCCTCTATTT TCCA***G***GAGAA CCAGGAGCCA
CAGCCGCGGC TCACGCCCCA CCGCAACAT TAAGATTACA AGTGGACACC TGAGTCAGCA GGACCCGGAA TCCCAGATGA GAGAGCTTAT
-94
CTACAC***G***ACT CAGATCTTGT TGTCACCCCC ATTATTGACA ATCCAAAGGT GCAGAAAGCA CTCTGACAAA TAATGAAACA ACCACCATCG
CHRFAM7A Open Reading Frame ‧ ‧ ‧ ‧ ‧ ‧ ‧ ‧ ‧ ‧ ▸
GTTAAATTTG ***ATG*** CAA AAA TAT TGC ATC TAC CAG CAT TTT CAG TTC CAA TTG CTA ATC CAG CAT TTG TGG ATA GCT
GCA AAC TGT GAT ATT GCT GAT GAG CGC TTT GAC GCC ACA TTC CAC ACT AA…

ion channel domain COOH   ion channel domain COOH

B Unique CHRFAM7A sequence

NH2–MQKYC IYQHF QFQLL
IQHLW IAANC DI...

(27 a.a. amino terminus)

C Two variants of human a7-nAChR (CHRNA7)

NH2–MRCS PGGVWLALAA SLLHGKATAS PPSTPPWDPG HIPGASVRPA
PGPVSLQGEF QRKLYKELVK NYNPLERPVA NDSQPLTVYF SLSLLQIMDV
DEKNQVLTTN IWLQMSWTDH YLQWNVSEYP GVKTVRFPDG QIWKPDILLY
NS...   (Variant 1: 110 a.a. & Variant 2: 146 a.a. amino terminus)

D Common C-terminus Channel Domain of CHRFAM7A and CHRNA7 (α7-nAChR, 384 a.a.)

.....ADERFDAT FHTNVLVNSS GHCQYLPPGI FKSSCYIDVR WFPFDVQHCK LKFGSWSYGG WSLDLQ***MQE***A DISGYIPNGE
WDLVGIPGKR SERFYECCKE PYPDVTFTVT MRRRTLYYGL NLLIPCVLIS ALALLVFLLP ADSGEKISLG ITVLLSLTVF
MLLVAEIMPA TSDSVPLIAQ YFASTMIIVG LSVVVTVIVL QYHHHDPDGG KMPKWTRVIL NWCAWFLRMK RPGEDKVRPA
CQHKQRRCSL ASVEMSAVAP PPASNGNLLY IGFRGLDGVH CVPTPDSGVV CGRMACSPTH DEHLLHGGQP PEGDPDLAKI
LEEVRYIANR FRCQDESEAV CSEWKFAACV VDRLCLMAFS VFTIICTIGI LMSAPNFVEA VSKDFA–COOH

Figure 2. Identification of *CHRFAM7A* in THP1 cells. (A) 5′ RACE of human THP1 cells identified 11 of 14 *CHRFAM7A* transcripts sequenced as initiating at –446 bp from the *CHRFAM7A* open reading frame (A of the ATG = +1). (B) Translation of the DNA sequence established that the deduced *CHRFAM7A* protein has a unique 27 amino acid sequence that distinguishes *CHRFAM7A* from the amino terminus of *CHRNA7*. The *CHRFAM7A* exons and the amino acid sequence they encode are shown in blue and red. (C) The *CHRNA7* gene encodes two protein variants that differ by the underlined sequence. (D) The common 386 amino acid sequence shared by both *CHRFAM7A* and *CHRNA7* also shows the sequence encoded by the variant 2 of *CHRFAM7A* which is 100% identical between both genes but not detected in the RT-PCR experiments described here or observed after 5′RACE of THP1 cells.

pression correlates with protein expression, then the data suggest the existence of significant heterogeneity in the CHRFAM7A–CHRNA7 pentamer that forms the human cell surface α7nAChR on human leukocytes.

CHRFAM7A Has a Unique and Distinct Promoter Regulating Gene Expression

Expression levels of *CHRFAM7A* and *CHRNA7* in leukocytes suggest their independent regulation. Furthermore the 5′ UTR sequence and the translation initiation site of the *CHRFAM7A* gene from the 5′ RACE analyses (see Figure 2) al-

lowed us to infer the existence of the CHRFAM7A variant 1 protein in human leukocytes that others have detected by immunoblotting with anti-*CHRNA7* antibodies (10,11). With these sequences, we used a bioinformatic approach to identify potential transcription factor binding sites (40) and experimental promoter mapping techniques to assess the regulation of *CHRFAM7A* gene expression. As illustrated in Figure 4A, five 5′ UTR plasmid constructs were prepared with DNA sequences that ranged from +22 to –2400 bp of the *CHRFAM7A* variant 1 transcript using the adenosine in

the ATG ORF as +1 (see Materials and Methods). Each 5′ UTR–containing plasmid was then tested for its ability to activate luciferase gene expression in transiently transfected THP1 cells (Figure 4B). Promoter activity was observed within 500 bp of the *CHRFAM7A* ORF. Interestingly, 5′ extensions of this fragment encode dominantly negative inhibitory sequences that decrease the luciferase activity observed within the first 500 bp of the 5′ UTR. These data point to the existence of both stimulatory and inhibitory transcriptional elements regulating *CHRFAM7A* gene expression, per-
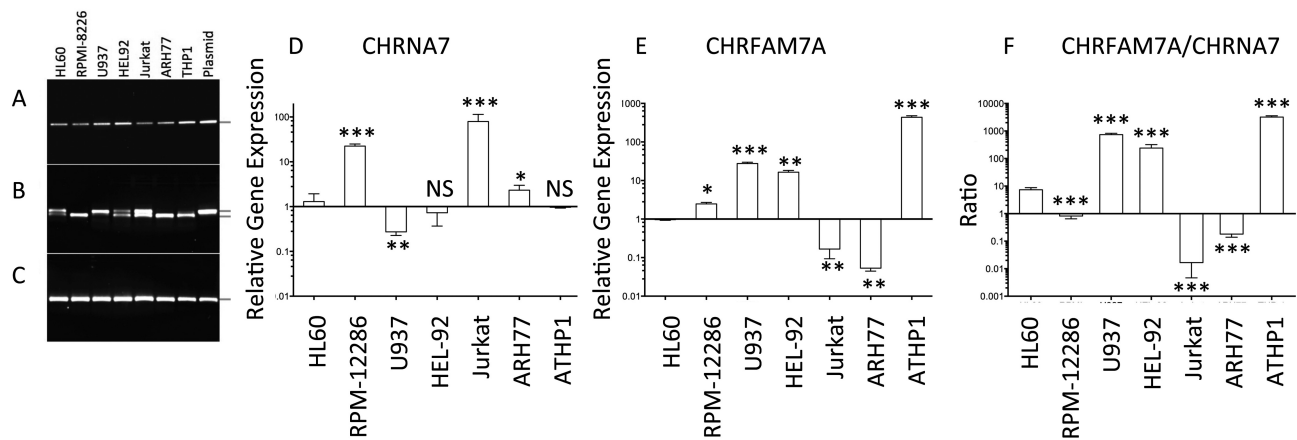
Figure 3. Regulation of *CHRNA7* and *CHRFAM7A* in leukocyte lines. mRNA was isolated from HL60, RPMI8226, U937, HEL92, Jurkat, ARH77 and THP1 cells and the cDNA prepared was probed for the presence of *CHRFAM7A* (A), *CHRNA7* (B) and *GAPDH* (C) by PCR. The amplicons were compared with that generated with their respective plasmids encoding variant 1 of human *CHRFAM7A*, variant 1 of human *CHRNA7* or human *GAPDH*. The differences in gene expression were quantified in cultures cells (N = 6) and are expressed as mean ± standard deviations after normalization to the levels of gene expression in HL60 cells (D and E). Significance of changes in gene expression was determined using the REST gene expression analysis program as described in Materials and Methods. The ratio of *CHRFAM7A:CHRNA7* gene expression (F) varies over 10,000-fold between different cell types (for example, Jurkat versus THP1). Significance of changes in the ratio of *CHRFAM7A:CHRNA7* gene expression was determined using Wilcoxon signed rank test of unpaired t test using the GraphPad PRISM 6.0. (*$p < 0.05$; **$p < 0.01$, ***$p < 0.001$)

haps reflecting its reported downregulation by LPS treatment in leukocytes (10,11) and differential upregulation in human epithelial cells (41).

Biological Consequence of *CHRFAM7A* Gene Expression in THP1 Cells

We used the transduction of THP1 cells with lentivirus to stably overexpress *CHRFAM7A* in THP1 cells and determine whether *CHRFAM7A* altered THP1 cell phenotype and/or gene expression. As shown in Figure 5, GFP-transduced THP1 cells (Figure 5A) can be differentiated from *CHRFAM7A*-transduced THP1 cells (Figure 5B) in that the latter tend to proliferate as loosely associated cell clusters that are reminiscent of expanding, transformed and presumably clonal cells. This is a marked contrast to the even distribution of both parental (not shown) and GFP-transduced THP1 cells, suggesting that *CHRFAM7A* overexpression affects cell–cell adhesion.

To assess the functional consequence of stable *CHRFAM7A* overexpression, we

used flow cytometry to first show that fluorescently labeled bungarotoxin (BT), a specific α7nAChR ligand, binds the leukocyte α7nAChR on THP1 cells (Figure 5C). BT is an irreversibly binding toxin that has been described extensively and shown to be a highly specific determinant of α7nAChR ligand binding. It also distinguishes the cell surface α7nAChR channel/receptor from other nicotinic receptors (42,43). As shown in Figure 5C, the addition of fluorescently labeled BT to THP1 cells produces a tenfold shift from baseline fluorescence labeling of THP1 cells that indicates the presence of the α7nAChR channel/receptor. This shift in BT binding was then compared between BT binding to GFP-vector and *CHRFAM7A*-transduced THP1 cells. As shown in Figure 5D, *CHRFAM7A*-transduced THP1 cells bind even more than labeled BT, suggesting that *CHRFAM7A* overexpression increases the α7nAChR channel and receptor at the THP1 cell surface. Quantitative analyses of the mean fluorescence intensity (MFI) in vector- and *CHRFAM7A*-transduced cells confirmed the signifi-

cance of this shift (Figure 5E). These data suggest that stable *CHRFAM7A* overexpression either increased BT binding by altering ligand binding of a heteropentameric complex or by regulating *CHRNA7* gene expression, thereby facilitating, not inhibiting, α7nAChR transport to the cell surface (3,9,12–14).

To further investigate the biological consequences of stable *CHRFAM7A* overexpression, its ability to increase α7nAChR dependent BT binding and induce a THP1 cell clumping phenotype, we isolated mRNA from both vector- and *CHRFAM7A*-transfected cells and analyzed their respective transcriptomes by RNA-seq. Clustering analyses of gene expression were performed using both DESeq (32) and CutDiff (36) analytical tools. In comparing the effects of *CHRFAM7A* and GFP-vector gene expression, DESeq identified 653 differentially expressed genes and 139 differentially expressed genes identified by Cuffdiff. The top 30 up- and downregulated differentially expressed genes are presented in Table 1 and sorted on the basis of the statistical
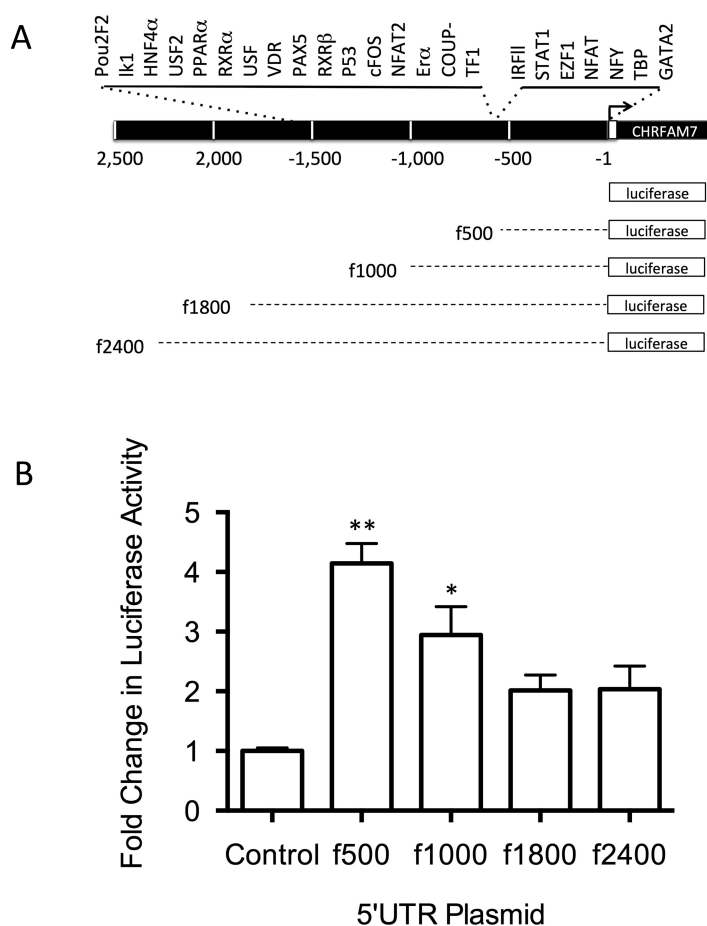
Figure 4. Regulation of *CHRFAM7A* expression. A schematic representation of 5' UTR *CHRFAM7A* (A) shows the potential transcription factor binding sites identified by consensus sequence analyses. The f2400-, f1800-, f1000- and f500-bp fragments of the 5' UTR were prepared as described in the text and then tested for promoter activity by cloning sequences into the promoter reporter assay (see Materials and Methods). Transient transfection of THP1 cells (B) showed luciferase expression upregulated by the f500 fragment in THP1 cells but translation inhibitory elements are detected in further 5' extensions of the 5' UTR *CHRFAM7A*. Statistical differences were analyzed by ANOVA (**$p < 0.01$; *$p < 0.05$; N = 6).

significance of differential gene expression. As expected, the highest differentially expressed gene was *CHRFAM7A* (55.4-fold) in the *CHRFAM7A*-transduced cells. It is particularly noteworthy however that an increase in *CHRNA7* expression (13.3-fold) was the second most significant difference in these stably transfected *CHRFAM7A* cells. This suggests that increased BT binding in *CHRFAM7A* cells (see Figure 5D) is the result of increased α7nAChR on the cell surface, rather then a reflection of an increase in a *CHRFAM7A* subunit in stably transfected cells. These data support the hypothesis that long-term and stable expression of *CHRFAM7A* modulates *CHRNA7* availability to the surface. Alternatively, the CHRFAM7A protein may form a human-specific α7nAChR heteropentamer at the leukocyte cell surface with modified ligand specificity, tropism and binding kinetics, compared with the α7nAChR homopentamer found in all species (3,9,12–14).

Among other significantly changed differential genes, versican (#1, 4.5-fold), tensin-like protein (#4, 8.7-fold), *SIGLEC1* (#7, 3.6-fold), glipican 6 (#15, 5.1-fold) and *EPSTI1* (#18, 3.3-fold) expression all tie to cell adhesion, which itself is a phenotypic difference between stable *CHRFAM7A*- and GFP-transduced cells (Figure 5). Interestingly, there are also two genes encoding antisense (PAX-AS1) and microRNA with differential expression that are nearly as high (44.3- and 40.6-fold) as the 55-fold change elicited by the *CHRFAM7A* transgene. Finally, it is also interesting to note that six of the most significantly altered genes are tied to interferon activity including *IFI6* (#5), *IFI44* (#6), *IFIT2* (#11) *IF44L* (#13), *IFIT1* (#14) and *IFI27* (#19).

We use GO enrichment analyses of the gene expression changes induced by stable *CHRFAM7A* expression to assess biological processes, cellular components and molecular functions (see Materials and Methods). As presented in Table 2, the most significantly enriched GO terms in each of the up- and down-regulated differentially expressed genes included the Type L interferon pathway, immune system processes and changes in cell adhesion. The latter is compatible with the phenotypic change detected microscopically. KEGG pathway assessments were used in a second test of differential gene expression and the most affected genes attributed to known pathways of cancer, leukocyte transendothelial migration and focal adhesion (Table 3 and Supplementary Figures S1, S2, S3).

DISCUSSION

Most genes are shared among all species but taxonomically restricted genes are only found in the genomes of specific taxa (for example, primates) and still others are species-specific, for example those uniquely localized to the human genome (29,44–52). While the emergence of human-specific genes is neither new nor unexpected, historically their study has been the focus of evolu-
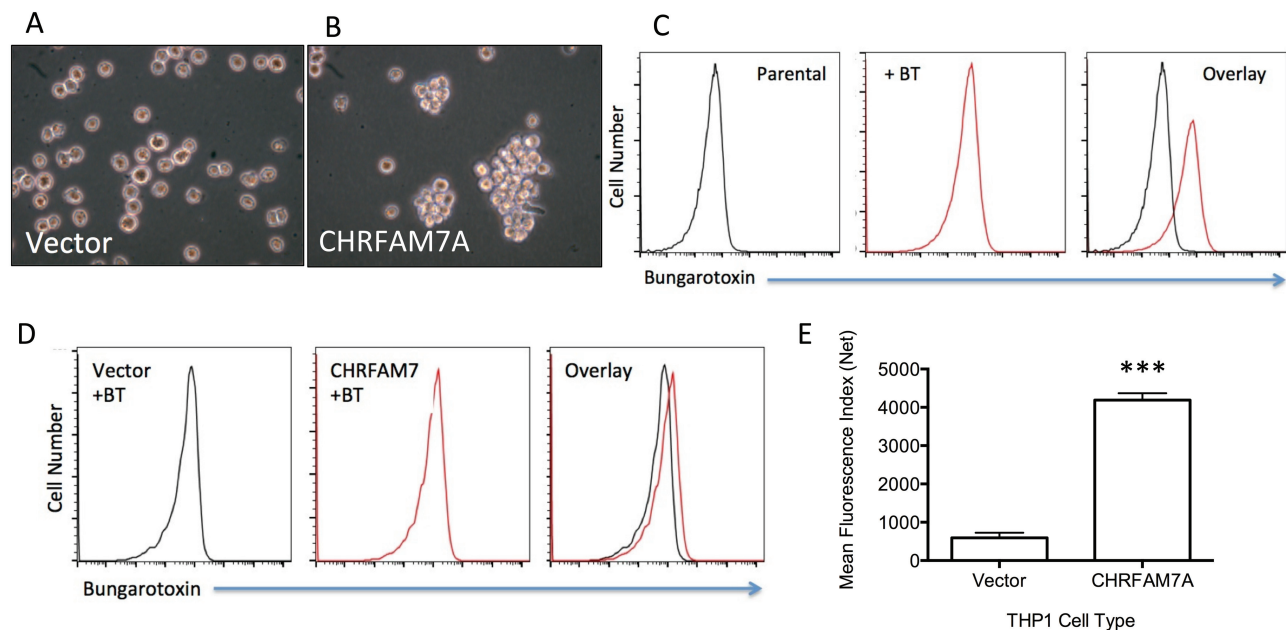
Figure 5. Biological consequences of *CHRFAM7A* expression. THP1 cells appear as characteristic mononuclear cells growing in suspension (A) but with stable *CHRFAM7A* overexpression (B) the THP1 cells display an increased cell-cell adhesion phenotype demonstrating that *CHRFAM7A* is biologically active and alters THP1 cells. As shown in (C), parental THP1 cells bind the selective α7nAChR agonist bungarotoxin (BT) which can be measured by flow cytometry of THP1 cells incubated with labeled BT. Similar flow cytometry after stable transduction of THP1 cells with *CHRFAM7A* showed increased BT binding (D) when compared with THP1 cells transfected with only GFP. The difference in specific bungarotoxin binding can be quantified by measuring the increase in mean fluorescence (E). (***$p <$ 0.001, N = 4)

tionary biologists interested in the human-specific biology that relates to cognition, behavior, reproduction and mental health (30,53,54). Interestingly, the existence of human-specific genes is rarely invoked to explain unexpected human inflammatory responses to disease. Yet, human immunity is highly adaptive to the environment, the human inflammatory response is both highly plastic and highly significant to species survival, particularly after injury.

To date, there are more than 300 human-specific genes that have been identified, although their number, identity and significance remain contentious (30,31). Generally, these genes are thought to arise from segmental duplication of previously existing genes, human-specific alternative splicing that creates new open reading frames regulated by cognate promoters, mutational events during humanoid evolution or through the endogenization of integrated viral se-

quences (55–57). The evolutionary advantages that these changes confer drive their retention and presumably their activities outweigh "off-target" effects that might mediate disease. In hominid evolution, one such selection is likely tracked to burn injury and the control of fire, which is a uniquely human activity that dates back some 3 million years. To this end, it is interesting to note that it is controversial as to whether or not animal models mimic the programmed inflammatory response to burn injury (58,59).

In support of the existence of unexpected and off-target consequences to the emergence of new genes, newly evolved genes appear to be represented disproportionately in gene sets associated with complex diseases when they are compared with older and more evolutionarily conserved genes (31). Thus, it is thought that human-specific genes might confer subtle but differential responsiveness to human cells when compared

with other species (60–62). Ironically, the absence of these human-specific genes in the genomes of animal models makes it impossible to study their contribution to human disease. *CHRFAM7A* is a case in point. It contributes human-specific activities that are tied to a widely distributed nicotinic ligand-gated ion channel called α7nAChR (*CHRNA7*) that plays a central role as a neurotransmitter receptor in the nervous system and in the regulation of inflammation.

The studies presented here are the first to establish a clear and unambiguous functional consequence to stable *CHRFAM7A* gene overexpression in a human leukocyte cell line. RNAseq of these stably transduced cells demonstrated increased *CHRNA7* gene expression and increased bungarotoxin binding, which differs from the reported effects of transient overexpression (12–14). While the significance of this difference is not known, the studies estab-

Table 1. Top differentially up- and downregulated genes, sorted by significance of change.

	Ensmbl	Entrez	Gene	Gene name or description	Δ	*p*
				Upregulated genes		
1	ENSG00000038427	1462	VCAN	Versican	4.5	7.40E-17
2	ENSG00000175344	1139	CHRNA7	Cholinergic receptor, nicotinic, α7 (neuronal)	13.3	2.50E-15
3	ENSG00000189223	654433	PAX8-AS1	PAX8 antisense RNA 1	44.3	2.80E-12
4	ENSG00000100181	387590	TPTEP1	Transmembrane phosphatase with tensin homology	8.7	8.20E-12
5	ENSG00000126709	2537	IFI6	Interferon, α-inducible protein 6	3.5	2.00E-11
6	ENSG00000137965	10561	IFI44	Interferon-induced protein 44	6.7	1.50E-09
7	ENSG00000088827	6614	SIGLEC1	Sialic acid binding Ig-like lectin 1, sialoadhesin	3.6	3.80E-09
8	ENSG00000166664	89832	CHRFAM7A	Transfected gene	55.4	7.80E-09
9	ENSG00000166104	102466227	MIR7162	Micro RNA 7162	40.6	9.50E-07
10	ENSG00000105655	51477	ISYNA1	Inositol-3-phosphate synthase 1	9.1	1.70E-06
11	ENSG00000119922	3433	IFIT2	Interferon-induced protein tetratricopeptide repeats 2	3.6	2.20E-06
12	ENSG00000206337	10866	HCP5	HLA complex P5	12	6.40E-06
13	ENSG00000137959	10964	IFI44L	Interferon-induced protein 44-like	4.9	4.00E-05
14	ENSG00000185745	3434	IFIT1	Interferon-induced protein tetratricopeptide repeats 1	3.9	5.20E-05
15	ENSG00000183098	10082	GPC6	Glypican 6	5.1	6.30E-05
16	ENSG00000170365	4086	SMAD1	SMAD family member 1	3.8	8.90E-05
17	ENSG00000179796	116135	LRRC3B	Leucine rich repeat containing 3B	4.6	0.0002
18	ENSG00000133106	94240	EPSTI1	Epithelial stromal interaction 1	3.3	0.0002
19	ENSG00000165949	3429	IFI27	Interferon-induced protein 27	8.1	0.0006
20	ENSG00000081923	5205	ATP8B1	ATPase, aminophospholipid transporter, type 8b member 1	0.31	0.0006
				Downregulated genes		
	Ensmbl	Entrez	Gene	Gene name or description	Δ	*p*
21	ENSG00000174099	253827	MSRB3	Methionine sulfoxide reductase B3	0.37	1.80E-07
22	ENSG00000156515	3098	HK1	Hexokinase 1	0.42	8.60E-07
23	ENSG00000100060	4242	MFNG	MFNG O-fucosyl 3-β-N-acetylglucosaminyl-transferase	0.3	1.30E-06
24	ENSG00000100234	7078	TIMP3	TIMP metallopeptidase inhibitor 3	0.51	1.40E-06
25	ENSG00000182263	55137	FIGN	Fidgetin	0.08	3.30E-06
26	ENSG00000165659	1602	DACH1	Dachshund family transcription factor 1	0.46	1.50E-05
27	ENSG00000134824	9415	FADS2	Fatty acid desaturase 2	0.58	0.0002
28	ENSG00000126767	2002	ELK1	ELK1, member of ETS oncogene family	0.42	0.0002
29	ENSG00000144712	23066	CAND2	Cullin-associated and neddylation-dissociated 2	0.31	0.0006
30	ENSG00000011600	7305	TYROBP	TYRO protein tyrosine kinase binding protein	0.59	0.0007

lish a clear and unambiguous coregulatory link between *CHRFAM7A* and the α7nAChR neurotransmitter receptor encoded by *CHRNA7*. Furthermore, they may reflect the importance of the ratio of *CHRFAM7A* to *CHRNA7* at the leukocyte cell surface in regulating the inflammation response (Figure 6). Pathway analyses of the changes in gene expression in these cells using both GO and KEGG algorithms show that *CHRFAM7A* has functional effects on leukocytes that tie the neurotransmitter receptor to leukocyte adhesion, trafficking and transformation. These sequelae may be direct effects of *CHRFAM7A* expression or

indirect effects caused by downstream genes affected by *CHRFAM7A*.

In the experiments described here, we show that *CHRFAM7A* is normally expressed in human leukocytes (see Figures 1, 2) and at levels similar to those of *CHRNA7*. In view of its capacity to regulate α7nAChR activity after transient transfection *in vitro* (12–14), the data shown imply that *CHRFAM7A* has the potential to modulate human leukocyte function and by inference, α7nAChR-regulated inflammation (16). Interestingly, we also find that the stable transduction of *CHRFAM7A* increases basal expression of *CHRNA7*, thereby establishing the ex-

istence of a concomitant and compensatory response to high *CHRFAM7A* expression. These data point to the possibility that the ratio of *CHRFAM7A* and *CHRNA7* expression may be important in defining the human α7nAChR response. To that end, we also established the identity of the THP1 *CHRFAM7A* variant, deduced the amino acid difference that distinguishes it from α7nAChR and mapped a unique promoter that differentially regulates *CHRFAM7A* from *CHRNA7* in leukocytes (see Figure 4). Finally, we showed that stable *CHRFAM7A* expression affects several molecular pathways of cell function including cell

Table 2. Top five significantly enriched GO terms in differentially expressed genes.

	Enriched GO terms	*P* value	False discovery rate
Upregulated by *CHRFAM7A* (DESeq)	Type I interferon signaling pathway	6.93E-019	5.23E-015
	Cellular response to type I interferon	6.93E-019	5.23E-015
	Response to type I interferon	8.79E-019	5.23E-015
	Response to stimulus	7.83E-017	2.28E-013
	Defense response to virus	8.82E-017	2.28E-013
Upregulated by *CHRFAM7A* (Cuffdiff)	Response to chemical	1.44E-11	6.18E-008
	Response to organic substance	1.72E-11	6.15E-008
	Defense response	3.74E-10	1.11E-006
	Immune system process	2.07E-007	4.62E-006
	Biological regulation	2.08E-009	4.63E-006
Downregulated by *CHRFAM7A* (DESeq)	Molecular function	7.90E-011	1.41E-006
	Binding	1.61E-010	1.44E-006
	Cytosolic ribosome	8.17E-010	2.82E-006
	Cytosolic large ribosomal subunit	9.47E-010	2.82E-006
	Biological process	9.49E-010	2.82E-006
Downregulated by *CHRFAM7A* (Cuffdiff)	Calcium-dependent cell-cell adhesion	3.40E-005	1.59E-001
	Extracellular region	3.41E-005	1.59E-001
	Cell adhesion	3.54E-005	1.59E-001
	Biological adhesion	3.57E-005	1.59E-001
	Establishment of protein localization to membrane	1.07E-004	3.83E-001

adhesion, cell growth and cell trafficking. Inasmuch as there are no analogous or independently regulated *CHRFAM7A*-like genes in the genomes of other species (3,9), these findings implicate the existence of a human-specific mechanism in human leukocytes to gauge the human inflammatory response.

CONCLUSION

Together these data provide compelling evidence supporting the hypothesis that *CHRFAM7A* has a significant role in human leukocyte cell biology. *CHRFAM7A* has been shown to have the capacity to form cell surface heteropolymers with the wild-type α7nAChR (see Figure 6) and is reported in some models either to exert a dominant negative effect on α7nAChR, regulating the appearance of α7nAChR on the cell surface, or to alter ligand tropism (12–14). As a role for α7nAChRs in leukocyte homeostasis is unequivocal (16), *CHRFAM7A* might then confer leukocytes with a human-specific responsiveness to trophic stimuli that remains to be defined. In one example, efferent signaling of the vagus nerve has a central role in regulating inflammation and α7nAChR activation is an oblig-

atory intermediate, at least in mice (2,16–19,29,63,64). If the vagus nerve were presumed to have a similarly critical role in maintaining immune homeostasis in humans, then *CHRFAM7A* would likely gauge the immunomodulatory properties of human α7nAChR in a human-specific manner.

The human chromosome 15q13–14 locus contains the 10-exon human *CHRNA7* gene that encodes the α7 subunit of the prototypic homopentameric α7nAChR ligand-gated ion channel. This locus, however, also underwent significant rearrangement during human evo-

lution, leading to the emergence of the *CHRFAM7A* gene (reviewed in [3,9]). While the *CHRFAM7A* gene is structurally similar to *CHRNA7* (4), it has lost five *CHRNA7* exons and acquired five exons of a partially duplicated FAM7-UL kinase gene that was once on human chromosome 3. The in-frame fusion of these three partially duplicated genes led to the emergence of *CHRFAM7A* (3,9). Since its discovery in 1998 (4), numerous studies have shown that, like *CHRNA7*, *CHRFAM7A* is expressed in the central nervous system (CNS) and several genomic analyses have associated it and a

Table 3. Top five most significantly enriched KEGG pathways.

| Sample comparison	Enriched pathways	*P* value	False discovery rate
CHRFAM7A (DESeq)	Ribosome	3.35E-003	4.40E-001
	Pathways in cancer	5.68E-003	4.40E-001
	Hepatitis C	7.37E-003	4.40E-001
	Colorectal cancer	1.16E-002	5.20E-001
	Leukocyte transendothelial migration	1.78E-002	6.06E-001
CHRFAM7A (Cuffdiff)	Cytokine-receptor interactions	1.64E-002	4.05E-001
	Osteoclast differentiation	1.74E-002	4.05E-001
	RIG-I-like receptor signaling	1.78E-002	4.05E-001
	Insulin signaling pathway	2.23E-002	4.05E-001
	TGF-β signaling pathway	2.76E-002	4.05E-001
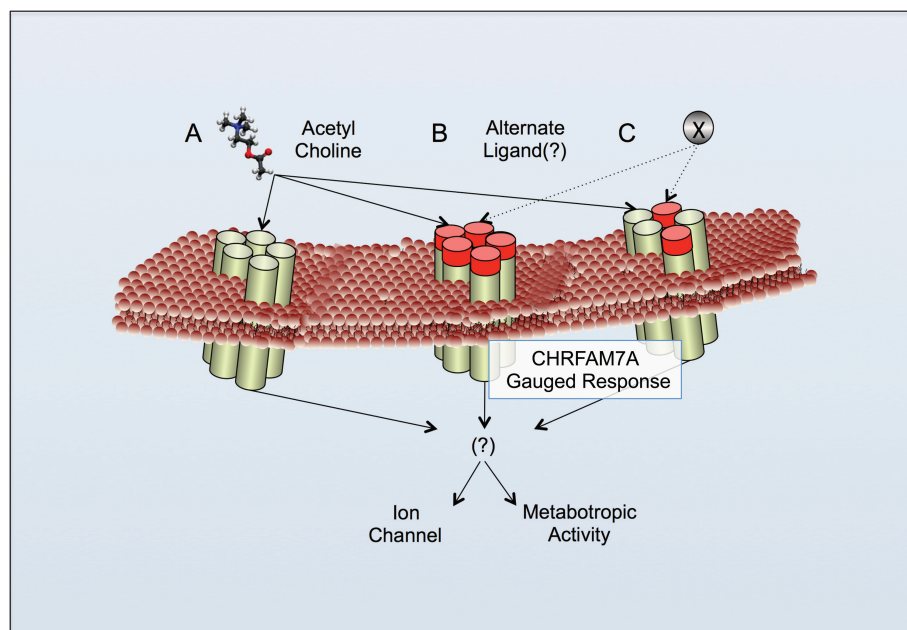
Figure 6. Specifying the human vagus-mediated inflammatory response. The identification of a gene encoding a human-specific subunit of α7nAChR raises the possibility that in humans, the canonical regulation of inflammation by vagus nerve may be mediated by cell surface α7nAChR homopentamers composed of *CHRNA7* (A) or *CHRFAM7A* (B) on human leukocytes or alternatively, heteropentameric receptors composed of a combination *CHRFAM7A* and *CHRFAM7A* subunits (C) The latter would alter ligand tropism, specificity, binding kinetics and cell responsiveness.

2-bp mutation with neuropsychiatric disorders including schizophrenia (65), bipolar disorder (66) and autism (67).

The natural ligand(s) responsible for *CHRFAM7A* activation is presumed to include acetylcholine, but its ligand selectivity is not known compared with other nAChRs, each of which have been described extensively (68). Normally, acetylcholine is thought to be the intrinsic ligand that activates the cell surface α7nAChR homopentameric channel, but there are numerous alternative ligands including choline, nicotine and even peptide hormone-like ligands (69–73) that can activate α7nAChR. The discovery of an alternative α7nAChR in human leukocytes raises the possibility that heteropentamers composed of CHRNA7 and CHRFAM7A proteins could modulate the cellular immune response to proinflammatory challenges (see Figure 6). In this way, the responsiveness of the nuclear factor kappa-B

(NF-κB) and Jak2/STAT3 inflammatory signaling pathways (74,75) that has been normally ascribed to the homopentameric product of *CHRNA7* may be altered by ligand binding to cells that express homopentameric *CHRFAM7A* or CHRNA7–CHRFAM7A heteropentamers on the cell surface. Interestingly, this subunit heterogeneity is well recognized for growth factors (for example, PDGF, activin and inhibin), receptors (for example, transforming growth factor [TGF]β, platelet-derived growth factor [PDGF] and fibroblast growth factor [FGF] receptors), integrins (for example, α/β/γ subunits) and other α/βAChR subunits from distinct genes. In the case of *CHRFAM7A*-encoded heteropentamers, they appear unique because *CHRFAM7A* only exists in the human genome and therefore, could define a currently unknown, human-specific response.

On a final note, it is worth noting that there is a mutagenized form of

CHRFAM7A that has been more extensively studied in mental health research on the presumption that *CHRFAM7A* might have evolved as an alternative ligand-gated ion-channel-regulating neuronal function (76–78). There are no studies describing the possible effect of this mutant gene on human leukocyte function, let alone the evolutionary pressures that originally led to the emergence, selection and retention of *CHRFAM7A* in humans. The findings presented here add to a growing body of evidence that collectively underscores the need to dissect the functional link between genes that arose for human speciation and the off-target emergence of complex human disease. In light of genetic analyses that associate newly emerged genes with complex disease, it is incumbent on investigators to use emerging models of human disease that can serve to study the contribution of human-specific disease. Just as mouse models were adapted specifically to study viruses with human-specific tropism (for example, HIV), analogous models will be needed to help determine the contribution of human-specific and taxonomically restricted genes to human biology, physiology and the pathobiology of human diseases tied to inflammation.

DISCLOSURE

The authors declare that they have no competing interests as defined by *Molecular Medicine*, or other interests that might be perceived to influence the results and discussion reported in this paper.

REFERENCES

1. Richman DP, Arnason BG. (1979) Nicotinic acetylcholine receptor: evidence for a functionally distinct receptor on human lymphocytes. *Proc. Natl. Acad. Sci. U. S. A.* 76:4632–5.

2. Cheadle GA, Costantini TW, Bansal V, Eliceiri BP, Coimbra R. (2014) Cholinergic signaling in the gut: a novel mechanism of barrier protection through activation of enteric glia cells. *Surg. Infect. (Larchmt.).* 15:387–93.

3. Sinkus ML, *et al.* (2015) The human CHRNA7 and CHRFAM7A genes: a review of the genetics, regulation, and function. *Neuropharmacology.* 96(Pt B):274–88.

4. Gault J, *et al.* (1998) Genomic organization and partial duplication of the human alpha7 neuronal nicotinic acetylcholine receptor gene (CHRNA7). *Genomics.* 52:173–85.

5. Zody MC, *et al.* (2006) Analysis of the DNA sequence and duplication history of human chromosome 15. *Nature.* 440:671–5.

6. Le Novere N, Corringer PJ, Changeux JP. (2002) The diversity of subunit composition in nAChRs: evolutionary origins, physiologic and pharmacologic consequences. *J. Neurobiol.* 53:447–56.

7. Locke DP, *et al.* (2003) Refinement of a chimpanzee pericentric inversion breakpoint to a segmental duplication cluster. *Genome Biol.* 4:R50.

8. Riley B, Williamson M, Collier D, Wilkie H, Makoff A. (2002) A 3-Mb map of a large Segmental duplication overlapping the alpha7-nicotinic acetylcholine receptor gene (CHRNA7) at human 15q13–q14. *Genomics.* 79:197–209.

9. Costantini TW, Dang X, Coimbra R, Eliceiri BP, Baird A. (2015) CHRFAM7A, a human-specific and partially duplicated alpha7-nicotinic acetylcholine receptor gene with the potential to specify a human-specific inflammatory response to injury. *J. Leukoc. Biol.* 97:247–57.

10. Villiger Y, *et al.* (2002) Expression of an alpha7 duplicate nicotinic acetylcholine receptor-related protein in human leukocytes. *J. Neuroimmunol.* 126:86–98.

11. Benfante R, *et al.* (2011) Expression of the alpha7 nAChR subunit duplicate form (CHRFAM7A) is down-regulated in the monocytic cell line THP-1 on treatment with LPS. *J. Neuroimmunol.* 230:74–84.

12. Araud T, *et al.* (2011) The chimeric gene CHRFAM7A, a partial duplication of the CHRNA7 gene, is a dominant negative regulator of alpha7*nAChR function. *Biochem. Pharmacol.* 82:904–14.

13. de Lucas-Cerrillo AM, *et al.* (2011) Function of partially duplicated human alpha77 nicotinic receptor subunit CHRFAM7A gene: potential implications for the cholinergic anti-inflammatory response. *J. Biol. Chem.* 286:594–606.

14. Wang Y, *et al.* (2014) The duplicated alpha7 subunits assemble and form functional nicotinic receptors with the full-length alpha7. *J. Biol. Chem.* 289:26451–63.

15. Tracey KJ. (2002) The inflammatory reflex. *Nature.* 420:853–9.

16. Tracey KJ. (2007) Physiology and immunology of the cholinergic antiinflammatory pathway. *J. Clin. Invest.* 117:289–96.

17. Tracey KJ. (2009) Reflex control of immunity. *Nat. Rev. Immunol.* 9:418–28.

18. Andersson U, Tracey KJ. (2012) Reflex principles of immunological homeostasis. *Annu. Rev. Immunol.* 30:313–35.

19. Olofsson PS, *et al.* (2012) alpha7 nicotinic acetylcholine receptor (alpha7nAChR) expression in bone marrow-derived non-T cells is required for the inflammatory reflex. *Mol. Med.* 18:539–43.

20. Olofsson PS, Rosas-Ballina M, Levine YA, Tracey KJ. (2012) Rethinking inflammation: neural circuits in the regulation of immunity. *Immunol. Rev.* 248:188–204.

21. Costantini TW, *et al.* (2010) Vagal nerve stimulation protects against burn-induced intestinal injury through activation of enteric glia cells. *Am. J. Physiol. Gastrointest. Liver Physiol.* 299:G1308–18.

22. Costantini TW, *et al.* (2010) Efferent vagal nerve stimulation attenuates gut barrier injury after burn: modulation of intestinal occludin expression. *J. Trauma.* 68:1349–54; discussion 1354–6.

23. Costantini TW, *et al.* (2012) Targeting alpha-7 nicotinic acetylcholine receptor in the enteric nervous system: a cholinergic agonist prevents gut barrier failure after severe burn injury. *Am. J. Pathol.* 181:478–86.

24. Lopez NE, *et al.* (2012) Vagal nerve stimulation decreases blood-brain barrier disruption after traumatic brain injury. *J. Trauma Acute Care Surg.* 72:1562–6.

25. Costantini TW, *et al.* (2009) Burn-induced gut barrier injury is attenuated by phosphodiesterase inhibition: effects on tight junction structural proteins. *Shock.* 31:416–22.

26. Costantini TW, *et al.* (2009) Role of p38 MAPK in burn-induced intestinal barrier breakdown. *J. Surg. Res.* 156:64–9.

27. Costantini TW, *et al.* (2009) Targeting the gut barrier: identification of a homing peptide sequence for delivery into the injured intestinal epithelial cell. *Surgery.* 146:206–12.

28. Matteoli G, *et al.* (2014) A distinct vagal anti-inflammatory pathway modulates intestinal muscularis resident macrophages independent of the spleen. *Gut.* 63:938–48.

29. Wang H, *et al.* (2003) Nicotinic acetylcholine receptor alpha7 subunit is an essential regulator of inflammation. *Nature.* 421:384–8.

30. Zhang YE, Long M. (2014) New genes contribute to genetic and phenotypic novelties in human evolution. *Curr. Opin. Genet. Dev.* 29:90–6.

31. Cooper DN, Kehrer-Sawatzki H. (2011) Exploring the potential relevance of human-specific genes to complex disease. *Hum. Genomics.* 5:99–107.

32. Anders S, Huber W. (2010) Differential expression analysis for sequence count data. *Genome Biol.* 11:R106.

33. Rapaport F, *et al.* (2013) Comprehensive evaluation of differential gene expression analysis methods for RNA-seq data. *Genome Biol.* 14:R95.

34. Zhou Y, Lin N, Zhang B. (2014) An iteration nor-malization and test method for differential expression analysis of RNA-seq data. *BioData Min.* 7:15.

35. Zhang ZH, *et al.* (2014) A comparative study of techniques for differential expression analysis on RNA-Seq data. *PloS One.* 9:e103207.

36. Trapnell C, *et al.* (2010) Transcript assembly and quantification by RNA-Seq reveals unannotated transcripts and isoform switching during cell differentiation. *Nat. Biotechnol.* 28:511–5.

37. Young MD, Wakefield MJ, Smyth GK, Oshlack A. (2010) Gene ontology analysis for RNA-seq: accounting for selection bias. *Genome Biol.* 11:R14.

38. Amarzguioui M, Prydz H. (2004) An algorithm for selection of functional siRNA sequences. *Biochem. Biophys. Res. Commun.* 316:1050–8.

39. Pfaffl MW, Horgan GW, Dempfle L. (2002) Relative expression software tool (REST) for group-wise comparison and statistical analysis of relative expression results in real-time PCR. *Nucleic Acids Res.* 30:e36.

40. Cartharius K, *et al.* (2005) MatInspector and beyond: promoter analysis based on transcription factor binding sites. *Bioinformatics.* 21:2933–42.

41. Dang X, Eliceiri BP, Baird A, Costantini TW. (2015) CHRFAM7A: a human-specific alpha7-nicotinic acetylcholine receptor gene shows differential responsiveness of human intestinal epithelial cells to LPS. *FASEB J.* 29:2292–302.

42. Marks MJ, Collins AC. (1982) Characterization of nicotine binding in mouse brain and comparison with the binding of alpha-bungarotoxin and quinuclidinyl benzilate. *Mol. Pharmacol.* 22:554–64.

43. Orr-Urtreger A, *et al.* (1997) Mice deficient in the alpha7 neuronal nicotinic acetylcholine receptor lack alpha-bungarotoxin binding sites and hippocampal fast nicotinic currents. *J. Neurosci.* 17:9165–71.

44. Chimpanzee S, Analysis C. (2005) Initial sequence of the chimpanzee genome and comparison with the human genome. *Nature.* 437:69–87.

45. Hedlund M, *et al.* (2007) N-glycolylneuraminic acid deficiency in mice: implications for human biology and evolution. *Mol. Cell. Biol.* 27:4340–6.

46. Huang H, *et al.* (2004) Evolutionary conservation and selection of human disease gene orthologs in the rat and mouse genomes. *Genome Biol.* 5:R47.

47. Knowles DG, McLysaght A. (2009) Recent de novo origin of human protein-coding genes. *Genome Res.* 19:1752–9.

48. Long M, Betran E, Thornton K, Wang W. (2003) The origin of new genes: glimpses from the young and old. *Nat. Rev. Genet.* 4:865–75.

49. Long M, *et al.* (2003) Origin of new genes: evidence from experimental and computational analyses. *Genetica.* 118:171–82.

50. Nahon JL. (2003) Birth of 'human-specific' genes during primate evolution. *Genetica.* 118:193–208.

51. Stahl PD, Wainszelbaum MJ. (2009) Human-specific genes may offer a unique window into human cell signaling. *Sci. Signal.* 2:pe59.

52. Tu Z, *et al.* (2006) Further understanding human disease genes by comparing with housekeeping genes and other genes. *BMC Genomics.* 7:31.

53. Zhang YE, Landback P, Vibranovski M, Long M. (2012) New genes expressed in human brains: implications for annotating evolving genomes. *Bioessays*. 34:982–991.

54. Zhang YE, Landback P, Vibranovski MD, Long M. (2011) Accelerated recruitment of new brain development genes into the human genome. *PLoS Biol.* 9:e1001179.

55. Redon R, *et al.* (2006) Global variation in copy number in the human genome. *Nature*. 444:444–54.

56. Waterston RH, Lander ES, Sulston JE. (2002) On the sequencing of the human genome. *Proc. Natl. Acad. Sci. U. S. A.* 99:3712–6.

57. Bailey JA, Eichler EE. (2006) Primate segmental duplications: crucibles of evolution, diversity and disease. *Nat. Rev. Genet.* 7:552–64.

58. Seok J, *et al.* (2013) Genomic responses in mouse models poorly mimic human inflammatory diseases. *Proc. Natl. Acad. Sci. U. S. A.* 110:3507–12.

59. Takao K, Miyakawa T. (2015) Genomic responses in mouse models greatly mimic human inflammatory diseases. *Proc. Natl. Acad. Sci. U. S. A.* 112:1167–72.

60. Davis MM. (2012) Immunology taught by humans. *Sci. Transl. Med.* 4:117fs112.

61. Liao BY, Zhang J. (2008) Null mutations in human and mouse orthologs frequently result in different phenotypes. *Proc. Natl. Acad. Sci. U. S. A.* 105:6987–92.

62. Mestas J, Hughes CC. (2004) Of mice and not men: differences between mouse and human immunology. *J. Immunol.* 172:2731–8.

63. Lowry DM, *et al.* (2014) The vagus nerve alters the pulmonary dendritic cell response to injury. *J. Surg. Res.* 192:12–8.

64. Morishita K, Costantini TW, Eliceiri B, Bansal V, Coimbra R. (2014) Vagal nerve stimulation modulates the dendritic cell profile in posthemorrhagic shock mesenteric lymph. *J. Trauma Acute Care Surg.* 76:610–7; discussion 617–8.

65. Freedman R, *et al.* (2001) Linkage disequilibrium for schizophrenia at the chromosome 15q13–14 locus of the alpha7-nicotinic acetylcholine receptor subunit gene (CHRNA7). *Am. J. Med. Genet.* 105:20–2.

66. Hong CJ, Lai IC, Liou LL, Tsai SJ. (2004) Association study of the human partially duplicated alpha7 nicotinic acetylcholine receptor genetic variant with bipolar disorder. *Neurosci. Lett.* 355:69–72.

67. Casey JP, *et al.* (2012) A novel approach of homozygous haplotype sharing identifies candidate genes in autism spectrum disorder. *Hum. Gen.* 131:565–79.

68. Wessler I, Kirkpatrick CJ. (2008) Acetylcholine beyond neurons: the non-neuronal cholinergic system in humans. *Br. J. Pharmacol.* 154:1558–71.

69. Arredondo J, Chernyavsky AI, Grando SA. (2006) Nicotinic receptors mediate tumorigenic action of tobacco-derived nitrosamines on immortalized oral epithelial cells. *Cancer Biol. Ther.* 5:511–7.

70. Arredondo J, Chernyavsky AI, Jolkovsky DL, Pinkerton KE, Grando SA. (2006) Receptor-mediated tobacco toxicity: cooperation of the Ras/Raf-1/MEK1/ERK and JAK-2/STAT-3 pathways downstream of alpha7 nicotinic receptor in oral keratinocytes. *FASEB J.* 20:2093–101.

71. Chernyavsky AI, Arredondo J, Galitovskiy V, Qian J, Grando SA. (2010) Upregulation of nuclear factor-kappaB expression by SLURP-1 is mediated by alpha7-nicotinic acetylcholine receptor and involves both ionic events and activation of protein kinases. *Am. J. Physiol. Cell Physiol.* 299:C903–11.

72. Papke RL. (2014) Merging old and new perspectives on nicotinic acetylcholine receptors. *Biochem. Pharmacol.* 89:1–11.

73. Papke RL, Chojnacka K, Horenstein NA. (2014) The minimal pharmacophore for silent agonism of the alpha7 nicotinic acetylcholine receptor. *J. Pharmacol. Exp. Ther.* 350:665–80.

74. de Jonge WJ, *et al.* (2005) Stimulation of the vagus nerve attenuates macrophage activation by activating the Jak2-STAT3 signaling pathway. *Nat. Immunol.* 6:844–51.

75. Yoshikawa H, *et al.* (2006) Nicotine inhibits the production of proinflammatory mediators in human monocytes by suppression of I-kappaB phosphorylation and nuclear factor-kappaB transcriptional activity through nicotinic acetylcholine receptor alpha7. *Clin. Exp. Immunol.* 146:116–23.

76. Sinkus ML, *et al.* (2009) A 2-base pair deletion polymorphism in the partial duplication of the alpha7 nicotinic acetylcholine gene (CHRFAM7A) on chromosome 15q14 is associated with schizophrenia. *Brain Res.* 1291:1–11.

77. Neri M, Bonassi S, Russo P. (2012) Genetic variations in CHRNA7 or CHRFAM7 and susceptibility to dementia. *Curr. Drug Targets.* 13:636–43.

78. Rozycka A, *et al.* (2013) Association study of the 2-bp deletion polymorphism in exon 6 of the CHRFAM7A gene with idiopathic generalized epilepsy. *DNA Cell Biol.* 32:640–7.

Cite this article as: Costantini TW, *et al*. (2015) A human-specific α7-nicotinic acetylcholine receptor gene in human leukocytes: identification, regulation and the consequences of *CHRFAM7A* expression. *Mol. Med*. 21:323–36.